to the International Atomic Energy Agency for their kind hospitality at the International Centre for Theoretical Physics at Trieste. All our numerical computations were performed on the IBM 7044 computer of Centro di Calcolo dell'Universita di Trieste.

APPENDIX: COMPONENT OF QUASIPARTICLE VACUUM IN FOUR-QP 0^+ QSTD SPURIONS

We compare the spectroscopic factors for the one-neutron stripping and pickup reactions on even and odd isotopes of tin calculated with the QSTD 0^+ eigenvectors obtained after projecting out the four-qp spurions $|\Psi_{sp4}'\rangle$ of Eq. (1) with those which result after projecting out the "usual" spurions $|\Psi_{sp4}\rangle$ of Eq. (22) of Ref. 3, i.e., including the qp-vacuum $|0\rangle$ components ($\langle 0|\Psi_{sp4}\rangle \neq 0$). From the comparison of the 0^+ QSTD energy levels of the present paper with those of Ref. 4 one can see that they are almost identical. The only difference is a very small depletion of the $|0\rangle$ component in $|0_1^+\rangle$ of the present paper.

In Table IV we compare the data of Refs. 14 and 15, respectively, with the spectroscopic factors $S_{\mathcal{J}}{}^{(+)}(0_1^+, \mathcal{J}_n{}^\pi)$ for the reaction $Sn^{116}(d,p)Sn^{117}$ and $S_{l=0}{}^{(-)}(0_n^+, \frac{1}{2}1^+)$ for the reaction $Sn^{117}(p,d)Sn^{116}$ calculated with the $|0_n^+\rangle$ eigenvectors of Sn^{116} corresponding to the two definitions of the four-qp spurions. We see that with the $|\Psi_{sp4}\rangle$ definition of the four-qp spurions ($\langle 0|\Psi_{sp4}\rangle \neq 0$) the calculated spectroscopic factors are in good over-all agreement with the data—not worse than that of the factors calculated with $|\Psi_{sp4}'\rangle(\langle 0|\Psi_{sp4}'\rangle = 0)$; in some cases of $\mathcal{J}_n{}^\pi$ the agreement is even better when one calculates with $|\Psi_{sp4}\rangle$.

TABLE IV. Comparison of the experimental spectroscopic factors of Schneid *et al.*[a] and Yagi *et al.*[b] for the reactions $Sn^{116}(d,p)$-Sn^{117} and $Sn^{117}(p,d)Sn^{116}$, with the spectroscopic factors calculated using the two different definitions of the four-qp spurions discussed in this paper.

$\mathcal{J}_n{}^\pi$	QSTD ($\langle 0\|\Psi_{sp4}'\rangle = 0$)	QSTD ($\langle 0\|\Psi_{sp4}\rangle \neq 0$)	Expt.	Reaction
$\frac{1}{2}1^+$	0.55	0.36	0.65	
$\frac{3}{2}1^+$	0.68	0.50	0.55	
$\frac{11}{2}1^-$	0.67	0.46	0.81	$Sn^{116}(d,p)Sn^{117}$
$\frac{7}{2}1^+$	0.31	0.16	0.13	
$\frac{5}{2}1^+$	0.12	0.07	0.061	
0_1^+	0.55	0.36	0.45	
0_2^+	0.38	0.38	0.087	$Sn^{117}(p,d)Sn^{116}$
0_3^+	0.02	0.02	0.092	

[a] Reference 14.
[b] Reference 15.

PHYSICAL REVIEW VOLUME 173, NUMBER 4 20 SEPTEMBER 1968

High-Resolution Gamma-Ray Spectroscopic Study of the Decay $^{133}Ba \rightarrow {}^{133}Cs$†

D. P. DONNELLY, J. J. REIDY, AND M. L. WIEDENBECK
Department of Physics, University of Michigan, Ann Arbor, Michigan 48104

(Received 4 March 1968)

The decay of ^{133}Ba to levels in ^{133}Cs was studied using Ge(Li) γ-ray spectrometers. The energies of the measured γ-ray transitions are 53.14(8), 160.68(10), 223.08(10), 276.45(8), 302.87(8), 355.99(7), and 383.92(7) keV. The corresponding relative γ-ray intensities of these transitions are 3.16(39), 0.99(10), 0.72(8), 11.62(82), 29.4(21), 100, and 14.3(10). γ-ray spectra in coincidence with the 53.1-, 79.6-, 81.0-, 276.4-, 302.9-, 356.0-, and 383.9-keV γ rays were obtained. The data are in quantitative agreement with the existing decay scheme. The K-shell internal-conversion coefficients were determined, using the present γ-ray relative intensities and published K-shell internal-conversion-electron relative intensities. These results and earlier lifetime measurements and mixing ratios were used to calculate γ-ray-transition retardation and enhancement factors.

1. INTRODUCTION

THE low-lying levels of ^{133}Cs are populated following the electron-capture decay of ^{133}Ba. From this decay, as well as from the decay of ^{133}Xe and Coulomb-excitation studies, much information has been obtained concerning the low-lying levels of ^{133}Cs. References to experimental studies of ^{133}Cs prior to 1967 have been given by Hennecke *et al.*[1]; more recent works are listed in Refs. 2–4. The main features of the decay scheme, consistent with recent work, are shown in Fig. 1. The levels were established in early work primarily on the basis of coincidence measurements. The first three levels have also been observed in Coulomb-excitation studies. The present spin assignments seem to be well established.

† Work supported in part by the U. S. Atomic Energy Commission.

[1] H. J. Hennecke, J. C. Manthuruthil, and O. Bergman, Phys. Rev. **159**, 955 (1967).

[2] A. Notea and Y. Gurfinkel, Nucl. Phys. **A107**, 193 (1968).

[3] H. E. Bosch, E. Szichman, A. Baseggio, and R. Dolinkue, Nucl. Instr. Methods **52**, 289 (1967).

[4] T. Paradellis, S. Hontzeas, S. I. H. Naqvi, and J. L. Wolfson, Bull. Am. Phys. Soc. **13**, 69 (1968).

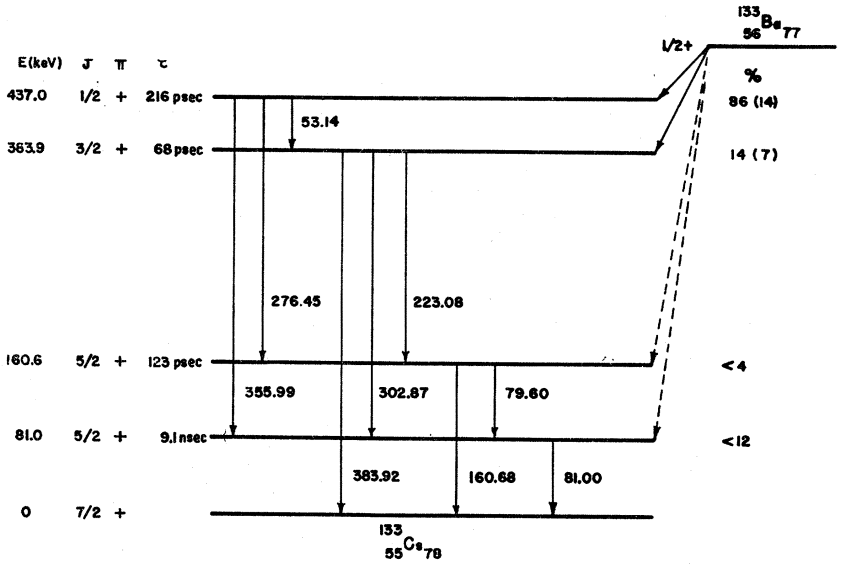

FIG. 1. Decay scheme of $^{133}Ba \rightarrow {}^{133}Cs$.

A high-resolution γ-ray spectroscopic study of this decay was made; energy and relative intensity values were determined, and coincidence measurements were performed. This complements recent high-resolution internal-conversion-electron studies[1,5] and assists in determining branching ratios, transition intensities, internal-conversion coefficients, and transition probabilities. With these results, additional features characteristic of the levels become evident.

2. EXPERIMENTAL

A. Apparatus

The Ge(Li) γ-ray spectrometer used in the energy and intensity measurements included the following components: an Ortec 4 $cm^2 \times 0.5$ cm Ge(Li) detector; a Tennelec TC-130 preamplifier and a TC-200 amplifier; and a Victoreen SCIPP 1600 multichannel analyzer. The TC-130 and TC-200 units were modified to include pole-zero cancellation. The γ-γ coincidence measurements utilized two Ge(Li) spectrometers. In addition to the one mentioned above a second Ge(Li) detector of active volume 8 $cm^2 \times 0.5$ cm was used in the gating channel. The coincidence spectra were measured with the Ge(Li) detectors oriented at 90°. A graded absorber was placed between the detectors to reduce crystal-to-crystal scattering. The coincidence measurements were taken utilizing crossover timing. The fast-coincidence circuit was operated with a resolving time of 50 nsec, and with a coincidence efficiency greater than 95% in the energy range investigated. The SCIPP analyzer was routed and coincidence spectra were taken in two 800-channel subgroups. Typical running times were 10^3 min, with coincidence counting rates of the order of 1 count/sec.

The calibration of the relative detection efficiency for the Ge(Li) detector used in this work is given in Ref. 6. Since that calibration did not include the energy region below 90 keV it was necessary to extend the calibration to lower energies. This was accomplished using a modified pair-point method. Instead of utilizing a source which yields a pair of γ rays with known emission rates, a source is used which involves de-excitation from only one level in the daughter nucleus. A comparison is then made of the relative peak areas of the γ ray and the x rays which follow the internal-conversion process. With a knowledge of the conversion coefficient and fluorescent yield, the "relative emission rates" can be determined. (If the source decays by electron capture, corrections must be made.) With this extension the calibration curve includes the energy region 20–3200 keV.

3. RESULTS

A. γ-Ray Energy Measurements

The energies of seven γ rays have been measured. The results of the energy measurements are shown in Table I along with γ-ray energies by Notea and

TABLE I. Energy values of ^{133}Cs γ rays.

γ-ray energy present work (keV)	Notea and Gurfinkel (keV)	Transition energy Thun *et al.* (keV)	Transition energy Hennecke *et al.* (keV)
53.14±0.08	53.4±0.25	53.17 ±0.04	53.152±0.020
		79.60 ±0.05	79.622±0.018
	81.1±0.26	80.997±0.006	80.990±0.022
160.68±0.10	160.5±0.27	160.66 ±0.06	160.58 ±0.04
223.08±0.10	223.2±0.45	223.43 ±0.26	223.15 ±0.05
276.45±0.08	276.5±0.32	276.43 ±0.26	276.35 ±0.05
302.87±0.08	303.0±0.63	303.09 ±0.21	302.78 ±0.05
355.99±0.07	356.3±0.48	356.26 ±0.15	355.92 ±0.06
383.92±0.07	384.1±0.42	384.09 ±0.20	383.79 ±0.07

[5] J. E. Thun, S. Törnkvist, K. Bonde Nielsen, H. Snellman, F. Falk, and A. Mocoroa, Nucl. Phys. 88, 289 (1966).

[6] D. P. Donnelly, H. W. Baer, J. J. Reidy, and M. L. Wiedenbeck, Nucl. Instr. Methods 57, 219 (1967).

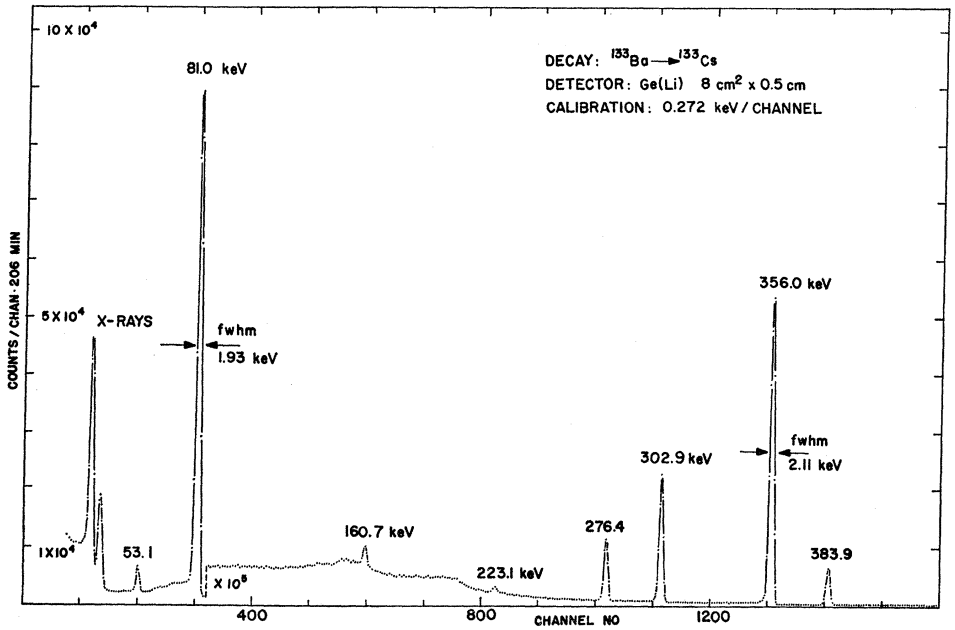

FIG. 2. γ-ray spectrum associated with the decay of $^{133}Ba \rightarrow {}^{133}Cs$.

Gurfinkel[2] and the transition energies from recent conversion-electron studies of Thun *et al.*[5] and of Hennecke *et al.*[1] The energies were determined by using an internal-calibration method; the centroid of the peak area was taken as the definition of the peak position (see Ref. 6). The errors include uncertainties in the energies of the calibration lines, peak positions, and electronic system nonlinearities.[6]

The 356-, 384-, and composite 80-keV lines were used as internal-calibration lines. The energies of the two highest energy lines were determined to be 355.99±0.07 and 383.92±0.07 keV by detecting, simultaneously, γ rays from the decays of $^{133}Ba \rightarrow {}^{133}Cs$, $^{51}Cr \rightarrow {}^{51}V$, and $^{198}Au \rightarrow {}^{198}Hg$. The energy of the most intense γ ray[7] in the decay $^{51}Cr \rightarrow {}^{51}V$ is 320.080±0.013 keV; in the decay $^{198}Au \rightarrow {}^{198}Hg$ it is 411.795±0.009 keV.[8] It is evident from the γ-ray spectrum in Fig. 2 that the photopeaks are sufficiently well resolved that there were no overlapping peaks when γ rays associated with the three above-mentioned decays were observed simultaneously. The current resolution of the Ge(Li) spectrometer would allow only indirect information about the lines near 80 keV; consequently, the composite peak from the sum of the 79.6- and 81.0-keV lines was used as a calibration for the low-energy end of the spectrum. By using the energies from Siegbahn *et al.*[9] and from Thun *et al.*[5] and the data of Bilger and Sherman[10] to estimate the relative intensities of the two γ rays, an energy for the composite peak was calculated to be 80.86±0.07. This value is relatively insensitive to changes in the intensity ratio of the two γ rays.

TABLE II. Relative intensity values of ^{133}Cs γ rays.

Energy (keV)	Relative γ-ray intensities: Present work[a]	Notea and Gurfinkel[b]	Thun *et al.* (1966)	Mann and Chaturvedi (1963)
53.2	3.16±0.39	3.78±0.09		2.5±1.0
79.6	5.48±0.71	4.9 ±0.59		52.0±2.0[c]
81.0	52.0 ±6.8	59 ±7.2		
160.7	0.99±0.10	1.21±0.05		
223.2	0.72±0.08	0.80±0.042		
276.4	11.62±0.82	11.6 ±0.17	11.0	10.0±1.0
302.9	29.4 ±2.1	29.7 ±0.29	25.8	21.0±2.0
356.0	100.0	100	100.0	100.0
383.9	14.3 ±1.0	14.1 ±0.26	14.7	11.0±3.0

[a] Errors include uncertainty in the detection-efficiency calibration.
[b] Errors quoted are 1 standard deviation of the mean.
[c] Sum of the 80- and 81-keV transition intensities.

[7] J. J. Reidy (private communication).
[8] G. Murray, R. L. Graham, and J. S. Geiger, Nucl. Phys. **45**, 177 (1963).

B. γ-Ray Relative-Intensity Measurements

The γ-ray relative intensities were determined by using the relative full-energy peak detection efficiency curve described in Ref. 6 and the extension of that curve discussed above in Sec. 2. The results of the relative-intensity measurements are shown in Table II along with the results of Notea and Gurfinkel,[2] Thun *et al.*,[5] and Mann and Chaturvedi.[11] The errors in the relative-intensity measurement include both the uncertainties in the measurement of the peak areas and the uncertainties in the detection-efficiency curve. The intensity of the 79.6 relative to the 81.0-keV line was estimated from the

[9] K. Siegbahn, C. Nordling, S.-E. Karlsson, S. Hagström, A. Fahlman, and I. Andersson, Nucl. Instr. Methods **27**, 173 (1964).
[10] H. R. Bilger and I. S. Sherman, Phys. Letters **20**, 513 (1966); and (private communication).
[11] K. C. Mann and R. P. Chaturvedi, Can. J. Phys. **41**, 932 (1963).

data of Bilger and Sherman.[10] This information, used in conjunction with the relative intensity of the composite peak, allowed a determination of the intensity of the two peaks relative to the 356-keV line.

A careful search for a 437-keV transition was made, and an upper limit on its γ-ray transition strength was set at 0.06% of the 356-keV γ-ray-transition intensity. In this decay there are several combinations of γ rays which sum to 437 keV, the 356+81, 384+53, and 276+80+81 combinations being the strongest. To prevent summing, a cadmium sheet was placed in front of the detector which absorbed the γ rays at 53 keV to the extent that no peak was visible at that energy and the intensity of the 80-keV peak relative to the 356-keV line was reduced by a factor of about 40. No peak was observed at an energy of 437 keV, and an upper limit was placed on its strength.

Internal K-shell conversion coefficients were calculated using the present γ-ray relative-intensity measurements and the relative K-shell internal-conversion electron intensities of Thun *et al.*[5] and of Hennecke *et al.*[1] These calculations were normalized so that the $\alpha_K(356)$ was set equal to the theoretical $E2$ value for this transition calculated by Sliv and Band.[12] The data supporting the $E2$ character of the 356-keV transition are L-subshell measurements and $K/L+M$ ratios.[1,13] The results are shown in Table III together with the conversion coefficients of Thun *et al.*[5] and of Mann and Chaturvedi.[11]

TABLE III. K-shell conversion coefficients.

Transition energy (keV)	Present γ intensities; average of electron intensities[a]	Thun *et al.*[b]	Mann and Chaturvedi[c]	Theoret.[d] $M1$	Theoret.[d] $E2$
53.2	5.56 ±1.26			4.89	6.6
79.6	1.06 ±0.22	1.36 ±0.10		1.50	2.4
81.0	1.28 ±0.23	1.36 ±0.10		1.42	2.26
160.7	0.30 ±0.11	0.39 ±0.13		0.203	0.266
223.1	0.76 ±0.012			0.083	0.092
276.4	0.046±0.006	0.050±0.008	0.047	0.047	0.045
302.9	0.037±0.005	0.037±0.006	0.036±0.004	0.037	0.034
356.0	0.021	0.021	0.021±0.002	0.024	0.021
383.9	0.017±0.002	0.017±0.004	0.020±0.013	0.020	0.017

[a] Taken from Refs. 1 and 5.
[b] Reference 5.
[c] Reference 11.
[d] Interpolated from the tables of Sliv and Band (Ref. 12).

C. γ-γ Coincidence Measurements

The results of γ-γ coincidence measurements are presented below. All coincidence spectra shown in Figs. 3–6 have had accidentals subtracted. The method by which the amount subtracted was normalized is given below. The gated region for each coincidence run is shown in an insert with each coincidence spectrum.

From a measurement of the K/L capture ratio to the 437-keV level, the Q value has been determined to be about 500 keV.[5,14,15] Consequently, when the γ rays at 276 keV or above are gated, the accidentals may be subtracted by normalizing on the peaks at 276 keV and above.

Gate: 384-keV γ ray. The spectrum in coincidence with the 384-keV γ ray is shown in Fig. 3. Lines at 53 and 80 keV are visible in the coincidence spectrum.

Gate: 356-keV γ ray. The spectrum in coincidence with the 356-keV γ ray is shown in Fig. 3. The only γ-ray line in the coincidence spectrum is at 80 keV.

Gate: 303-keV γ ray. The spectrum in coincidence with the 303-keV γ ray is shown in Fig. 4. The lines in coincidence with the 303-keV γ-ray are at 53 and 80 keV. The intensity of the 80-keV line relative to the 53-keV line is 6.35.

Gate: 276-keV γ ray. The spectrum in coincidence with the 276-keV γ ray is shown in Fig. 4. Lines at 80 and 161 keV are in coincidence with the 276-keV γ ray. The intensity of the 80-keV line relative to the 161-keV line is 7.5.

Gate: 79-keV region. The spectrum in coincidence with the 79-keV region is shown in Fig. 5. Accidentals were subtracted by normalizing on the weak 384-keV line.[16] The lines seen in the coincidence spectrum are at 53, 80, 223, 276, 302, and 356 keV. The relative peak areas of the 223-, 276-, 302-, and 356-keV lines are 6.3:57:42:100. The peak position of the 80-keV line is shifted (relative to a singles spectrum) to a slightly higher energy.

Gate: 82-keV region. The spectrum in coincidence with the 82-keV region is shown in Fig. 5. Accidentals were subtracted by normalizing on the weak 384-keV line. The lines seen in the coincidence spectra are at 53, 80, 223, 276, 302, and 356 keV. The relative peak areas of the 223-, 276-, 302-, and 356-keV lines are 2.2:25:45:100. The peak position of the 80-keV line is shifted (relative to a singles spectrum) to a slightly lower energy.

Gate: 53-keV γ ray. The spectra in coincidence with the 53-keV γ ray plus Comptons and the Compton region around 59 keV are shown in Fig. 6. Accidentals were subtracted from the spectrum in coincidence with the 59-keV region by normalizing on the very weak 384-keV line. The normalization for the subtraction of accidentals from the spectrum in coincidence with the 53-keV line was determined by multiplying the number of accidentals for the spectrum in coincidence with the 59-keV region times the ratio of the gate counting rates.

On examination of the gates in Fig. 6, it is seen that the gate for the spectrum in coincidence with the 59-keV region has a contribution from the backscatter of

[12] L. A. Sliv and I. M. Band, in *Alpha-, Beta- and Gamma-Ray Spectroscopy*, edited by K. Siegbahn (North-Holland Publishing Co., Amsterdam, 1965), Vol. 2.
[13] L. D. Hendrick and F. T. Avignone, III, Phys. Rev. 158, 1181 (1967).
[14] G. Schulz, Z. Physik 203, 289 (1967).
[15] M. McDonnell and M. K. Ramaswamy, Bull. Am. Phys. Soc. 12, 1064 (1967).

[16] From the coincidence spectra already presented, it can be established that the (80)-keV lines are not in coincidence with the 384-keV line.

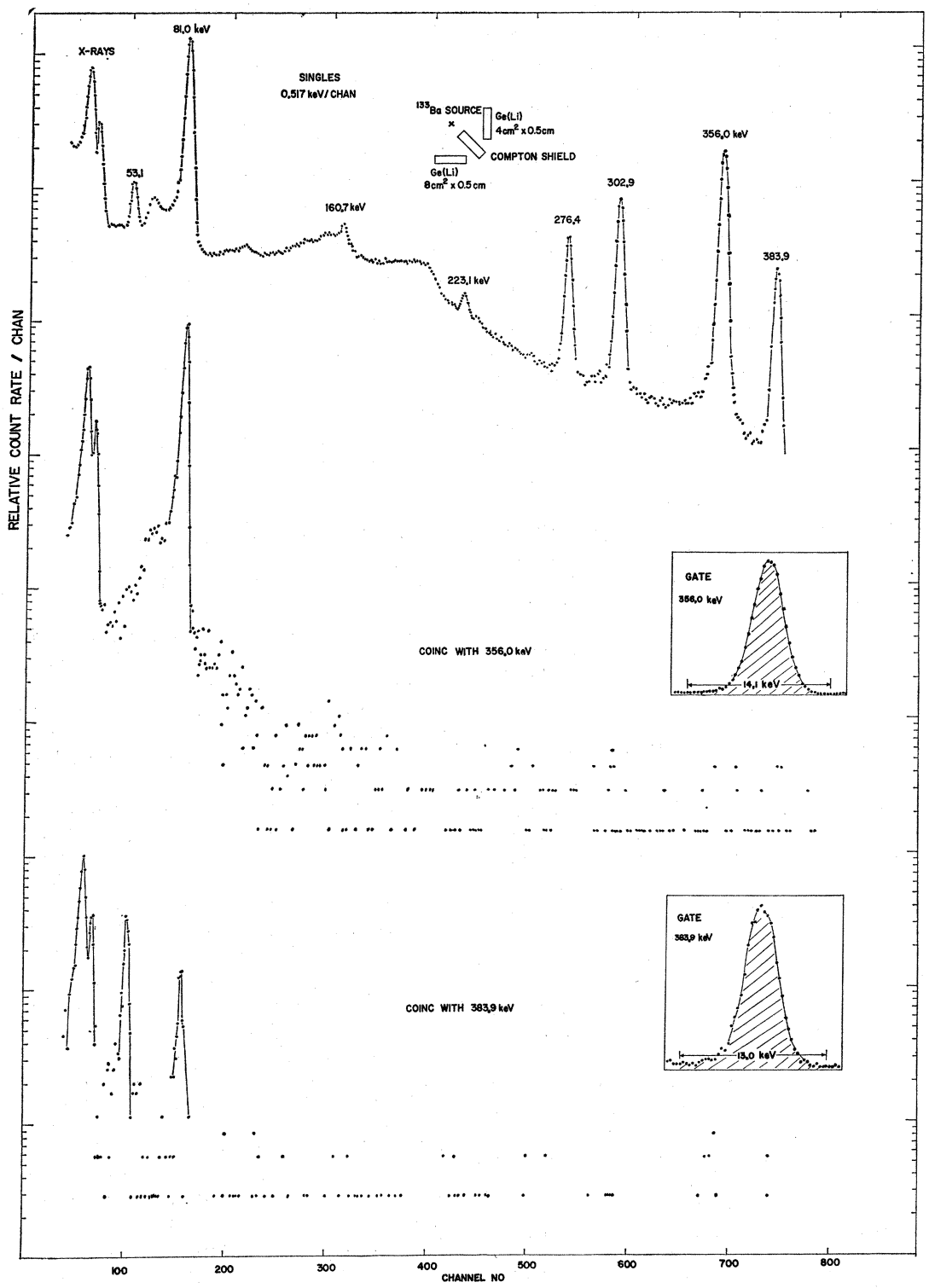

FIG. 3. γ-ray spectra in coincidence with the 356- and 384-keV γ rays.

the 81-keV γ rays which amounts to 10% of the gated region. This is not in the gate of the 53-keV γ ray. Consequently, the spectrum in coincidence with the 81-keV line, normalized to account for the backscatter, was subtracted from the spectrum in coincidence with the 59-keV region. This resulting spectrum was readjusted

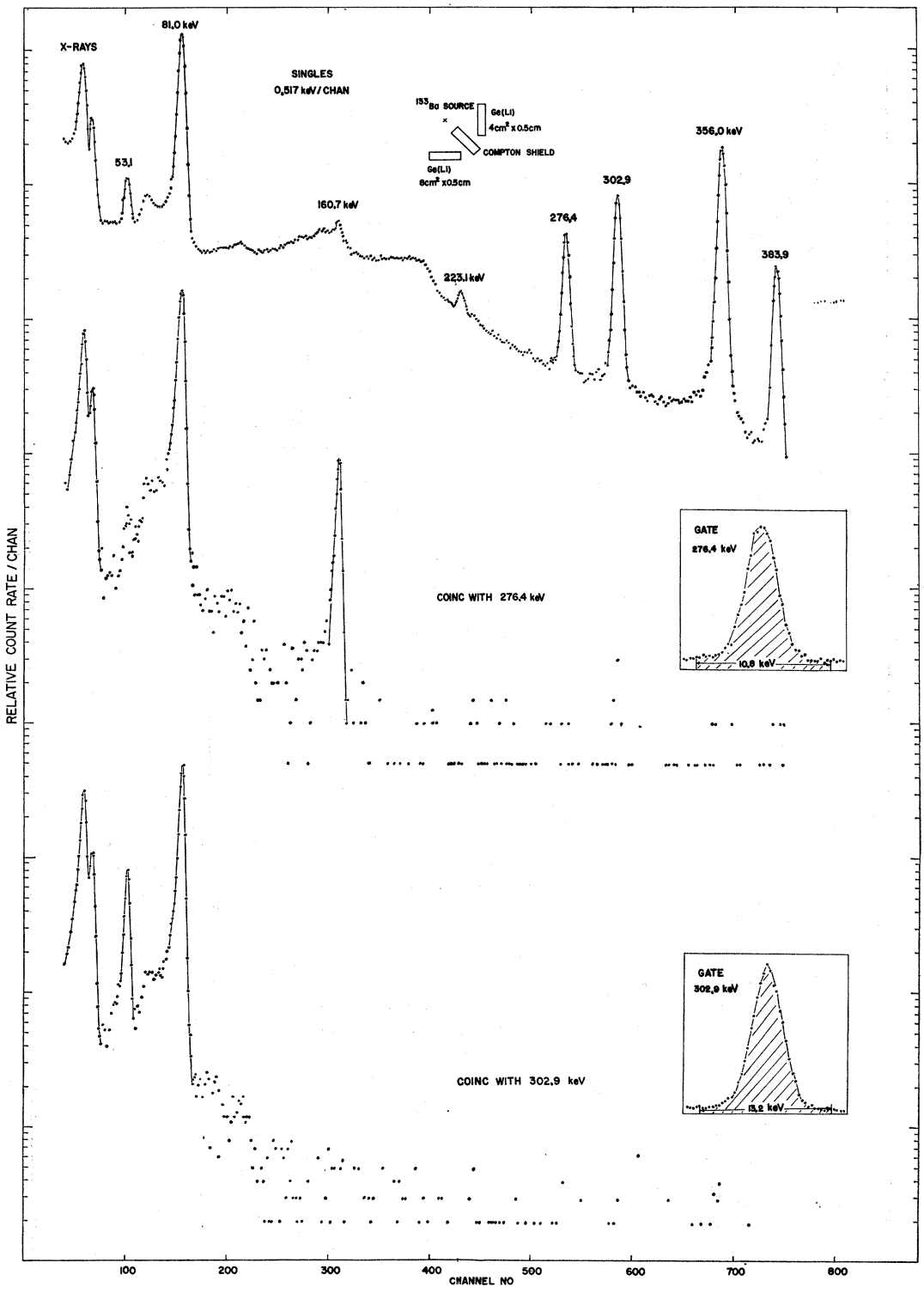

FIG. 4. γ-ray spectra in coincidence with the 276- and 303-keV γ rays.

to account for the difference in the gate widths of the 53 keV plus Comptons and 59-keV region and subtracted from the spectrum in coincidence with the 53-keV γ ray and Comptons. This final spectrum (not shown) indicates that lines at 80, 223, 302, and 384 keV are in coincidence with the 53-keV transition. After all

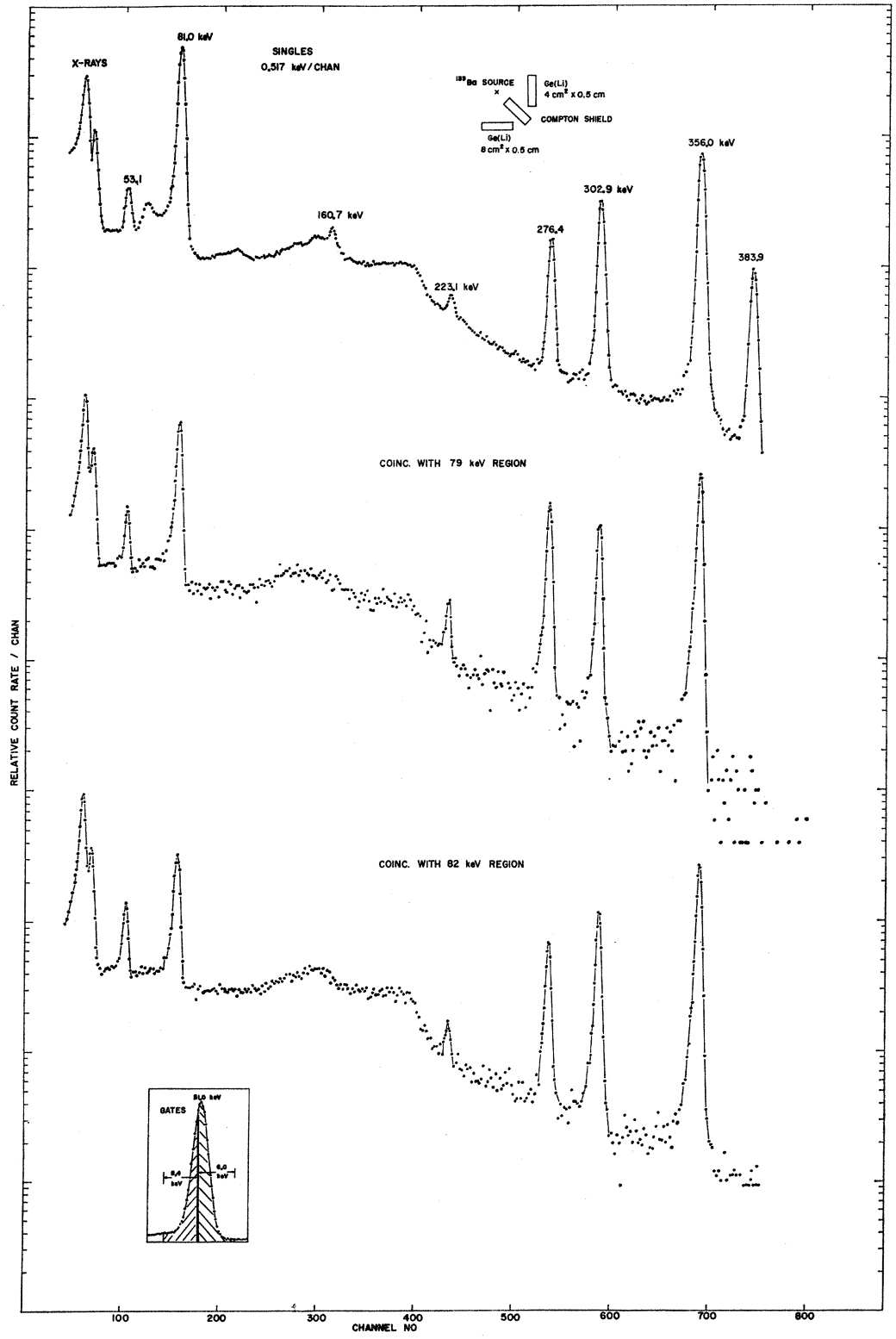

FIG. 5. γ-ray spectra in coincidence with the 79.6- and 81.0-keV γ rays.

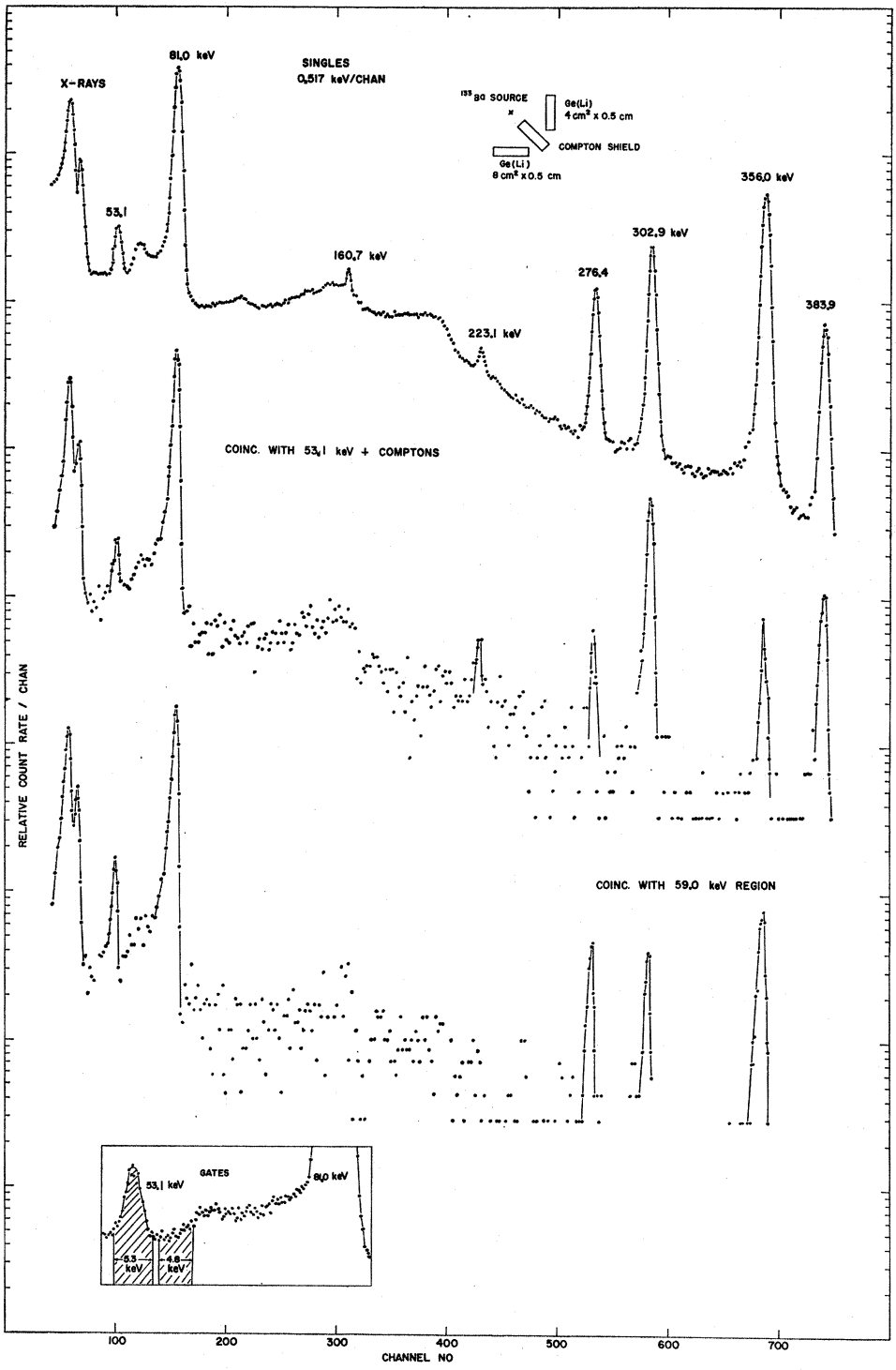

FIG. 6. γ-ray spectra in coincidence with the 53.1-keV γ-ray line and the 59-keV region.

the corrections, the ratios of the peak areas of the 223:303:384 γ rays are 2.8:41.7:11.1.

4. DECAY SCHEME AND DISCUSSION

A. Level Scheme

The level scheme in Fig. 1 is consistent with the transition energy measurements, the γ-γ coincidence results, and the fact that the first excited state has an excitation energy of 81 keV.[17–21]

The following sets of γ rays sum to 437 keV and have been observed in coincidence: 384 and 53 keV, 356 and (80) keV, 303, 53, and (80) keV, and 276 and 161 keV. This information places the 53-, (80)-, 303-, 356-, and 384-keV γ rays in the decay scheme as shown in Fig. 1.

It has been established previously[1,5] that the 80-keV line is a doublet. Coincidence runs which were made gating on the 79- and 82-keV regions confirm this fact. When gating on the 79- and 82-keV energy regions, the (80)-keV line in the coincidence spectrum is shifted (relative to a singles spectrum) to higher and lower energies, respectively. The 161-keV line is not visible in either coincidence spectrum and an (80)-keV line is in both coincidence spectra. In addition lines at 161 and (80) keV are in coincidence when gating the 276-keV line. These results indicate that the 161-keV line is the crossover transition for the 79.6- and 81.0-keV transitions and that the 276-, 161-, and 79.6-keV transitions are placed in the level scheme as indicated in Fig. 1. If the 79.6- and 81-keV transitions are placed correctly, then an increase should be observed in the intensities of the 223- and 276-keV lines relative to the 303- and 356-keV lines when gating the 79.6-keV γ-ray line. The relative full-energy peak areas of the 223-, 276-, 303-, and 356-keV lines in the singles spectrum are about 2:20:42:100. When the 82-keV region is gated, the ratios are 2.2:25:45:100, while the ratios for the 79-keV region are 6.3:57:42:100.

TABLE IV. Transition intensities and branching ratios.

Energy (keV)	Transition intensity	Branching-level ratio 161	384	437
53.2	15.0 ± 5.3			0.175±0.067
79.6	7.7 ± 2.7	0.90±0.05		
81.0	82.0 ±15.0			
160.7	0.85± 0.28	0.10±0.05		
223.1	0.48± 0.14		0.017±0.006	
276.4	7.6 ± 1.6			0.089±0.022
302.9	18.9 ± 3.9		0.67 ±0.076	
356.0	63.0 ±12.0			0.736±0.070
383.9	9.0 ± 1.7		0.317±0.076	

[17] P. Erman and Z. Sujkowski, Arkiv Fysik **20**, 209 (1961).
[18] L. W. Fagg, Phys. Rev. **109**, 100 (1958).
[19] G. M. Temmer and N. P. Heydenburg, Phys. Rev. **104**, 967 (1956).
[20] D. G. Alkhazov, K. I. Erokhina, and I. Kh. Lemberg, Izv. Akad. Nauk SSSR, Ser. Fiz. **28**, 1667 (1964) [English transl.: Bull. Acad. Sci. USSR Phys. Ser. **28**, 1667 (1964)].
[21] N. Imanishi, F. Fukuzawa, and M. Sakisaka, Nucl. Phys. **A101**, 654 (1967).

When the 53-keV γ ray is gated, the 80-, 223-, 303-, and 384-keV lines are in coincidence. Presumably the 161-keV transition is also in coincidence. It is not seen in the coincidence spectrum, however, since the 161-keV level is fed by the weak 223-keV transition and the depopulation of this level is principally through the 80-keV transition. The 276- and 356-keV transitions are absent, in agreement with the decay scheme. When the 53-keV γ-ray line is gated, it would be expected that the peak-area ratios for the 223-, 303-, and 384-keV γ rays should be in the same ratio as in a singles spectrum (2:42:12.2). After all the corrections noted in Sec. 3 C, the ratios are 2.8:42:11.

The 80-keV line which appeared when gating the 384-keV γ ray is not in coincidence with the 384-keV γ ray. Summing of the K x ray and the 356-keV γ ray occurred, and this sum was within the gate set for the 384-keV line. This small amount of an "effective" 356-keV γ ray in the gate accounts for the 81-keV peak.

The presence of the weak 53-keV γ-ray line which appeared when gating on the 276-keV line is due to Compton-scattered γ rays from the 303- and 384-keV transitions in the gated region.

B. Transition Intensities and Branching Ratios

The total transition intensities and branching ratios can be calculated from γ-ray intensity measurements, K-shell conversion coefficients, and $(L+M+N)/K$ ratios. The total intensity for a given transition is

$$N_{\text{tot}\ i}=N_{\gamma i}\{1+\alpha_K[1+(L+M+N)/K]\}_i.$$

The transition intensities and branching ratios are given in Table IV. The γ-ray intensities and the conversion coefficients are from the present work; the $(L+M+N)/K$ ratios are calculated from data in Refs. 1, 5, and 9. The normalization of the intensities was determined by setting the sum of the electron-capture feedings to the second, third, and fourth excited states equal to 100. This is equivalent to (and was actually determined by) saying that the sum of the transitions to the ground state and first excited state, the 81-keV transition excluded, is equal to 100. The electron-capture feeding to a given level was then calculated by taking the difference between the sums of the transition intensities feeding and depopulating the level. The values quoted for the feedings to the first and second excited states are the calculated values plus 1 standard deviation of that value. The electron-capture branching to the 437- and 384-keV levels was determined to be 86/14. The above branching ratios, together with K-shell conversion coefficients, $(L+M+N)/K$ ratios, and the relative intensity of the 53- and 81-keV γ rays from the spectrum in coincidence with the 303-keV γ ray indicate an electron-capture branching to the 437- and 384-keV levels of 83/17.

TABLE V. Transition rates.

Energy (keV)	Internal-conversion coeff. (tot)	Branching ratio	Multipole mixing ratio (δ)	Expt. mean life[a,b]	Weisskopf mean life ($M1$)[b]	$M1$ retardation	Weisskopf mean life ($E2$)[b]	$E2$ enhancement
53.2	6.5	0.174	0.2[c]	2.16(−10)[d]	1.06(−10)	97	2.36(−5)	100
			0.1[e]			22		25
79.6	1.29	0.898	$0.05\leq\leq 0.25$[c]	1.23(−10)[f]	6.3(−11)	≈ 5	6.29(−6)	≥ 50
81.0	1.58	1.0	−0.155[c]	9.1(−9)[g]	3.48(−11)	690	3.36(−6)	≈ 3–4
			0.173[e]					
160.7	0.33	0.102	0.59[c]	1.23(−10)[f]	4.46(−12)	485	1.09(−7)	18
			1.03[e]			740		35
223.1	0.088	0.017	0.4[e]	0.68(−10)[h]	1.59(−12)	3150	2.02(−8)	
276.4	0.058	0.088	3.0[e]	2.16(−10)[d]	5.01(−13)		4.15(−9)	≈ 1–2
302.9	0.044	0.666	0.11[e]	0.68(−10)[h]	6.35(−13)	170	4.38(−9)	
356.0	0.025	0.738	4.0[e]	2.16(−10)[d]	2.34(−13)		1.17(−9)	4
383.9	0.020	0.317	2.0[e]	0.68(−10)[h]	2.18(−13)		9.36(−10)	3

[a] Values are the mean lifetimes of the level in seconds.
[b] Numbers within the parentheses give the power of 10 by which the preceding number should be multiplied.
[c] Reference 5.
[d] Reference 27.
[e] Reference 1.
[f] Reference 28.
[g] Reference 25.
[h] Calculated from $B(E2)$ value given in Ref. 20; the calculated mean life given in Table I of Ref. 20 appears to be a misprint.

C. Spin Assignment to the 161-keV Level

Although the spins and parities of the levels of ^{133}Cs are now well established, there has been some evidence for $J\pi=\frac{3}{2}^+$ for the 161-keV state. This evidence is principally the reported 13% electron-capture branching to the 161-keV level from the ^{133}Ba $\frac{1}{2}^+$ ground state.[22] The corresponding $\log ft\approx 9$ appeared to exclude a second-forbidden transition. All the well-established second-forbidden transitions have $\log ft\geq 10.6$.[23] On the basis of the present intensity balance, a $\log ft\geq 9.5$ is required. A recent coincidence measurement by Schulz[14] indicates that $I_{EC}(161)/I(276\gamma)\geq 0.1$. This gives a $\log ft\geq 10.1$. Consequently, present measurements on electron-capture branching do not exclude a second-forbidden transition to the 161-keV level or a spin $\frac{5}{2}^+$ for that level.

The 276–161-keV $\gamma\gamma$ directional correlation measurements[24–26] strongly support the $\frac{5}{2}^+$ assignment. The A_2 and A_4 values from Refs. 24–26 were used as data for a computer program devised by Gove. His computer calculations show that the χ^2 value for the $\frac{1}{2}(D,Q)\frac{3}{2}(Q)\frac{7}{2}$ case is ≈ 500 times the χ^2 value for the $\frac{1}{2}(Q)\frac{5}{2}(D,Q)\frac{7}{2}$ case.

D. Transition Rates

The experimental transition rates and Weisskopf transition estimates are compared in Table V. The observed rates were calculated using the present branching ratios and conversion coefficients; the mixing ratios and half-lives were taken from published data.[1,5,20,25,27,28] The statistical factor is included in the Weisskopf estimates[29,30]; for the 80-keV transition ($\frac{5}{2}^+\rightarrow\frac{5}{2}^+$) the statistical factor was set equal to 1.

On the basis of the shell model one might expect the low-lying levels in the Cs isotopes to include the possible spin values $\frac{7}{2}$, $\frac{5}{2}$, $\frac{3}{2}$, $\frac{1}{2}$, and $\frac{11}{2}$. Since the first and second excited states both have spin $\frac{5}{2}$, it is of interest to compare γ-ray transition rates involved in the feeding and depopulating of these levels. The $E2$ enhancement factor for the transitions from the spin $\frac{1}{2}^+$ level to the spin $\frac{5}{2}^+$ levels are nearly equal and small (in disagreement with the predictions of Kisslinger and Sorenson[31]). The $M1$ retardation factors for the ground-state transitions from both $\frac{5}{2}^+$ levels are of the same order. Both transitions depopulating the 161-keV level have enhanced $E2$ components; one of these transitions, however, feeds the other $\frac{5}{2}^+$ level. The only transition with a fast $M1$ rate (retardation about 5) is the 79.6-keV transition connecting the two $\frac{5}{2}^+$ levels. These results indicate that any difference in the character of the $\frac{5}{2}^+$ levels is not strongly manifested in the γ-ray transition rates.

ACKNOWLEDGMENTS

The authors would like to thank Dr. N. B. Gove for computing the various angular-correlation spin combinations. One of us (D. D.) would like to thank Helmut Baer for his helpful comments.

[22] M. G. Stewart and D. C. Lu, Phys. Rev. **117**, 1044 (1960).
[23] N. B. Gove, in *Nuclear Spin-Parity-Assignments*, edited by N. B. Gove (Academic Press Inc., New York, 1966), p. 83; and (private communication).
[24] L. I. Yin and M. L. Wiedenbeck, Nucl. Phys. **54**, 86 (1964).
[25] E. Bodenstedt, H. J. Körner, and E. Matthias, Nucl. Phys. **11**, 584 (1959).
[26] F. Münnich, K. Fricke, and U. Wellner, Z. Physik **174**, 68 (1963).
[27] H. A. Vartapetian, A. G. Khudaverdia, and T. A. Garibian, Congr. Intern. Phys. Nucl. (Paris) **2**, 520 (1964).
[28] W. Flauger and H. Schneider, Atom. Energ. **8**, 453 (1963).
[29] J. M. Blatt and V. F. Weisskopf, *Theoretical Nuclear Physics* (John Wiley & Sons, Inc., New York, 1952).
[30] A. H. Wapstra, G. H. Nijgh, and R. van Lieshout, *Nuclear Spectroscopy Tables* (North-Holland Publishing Co., Amsterdam, 1959).
[31] L. S. Kisslinger and R. A. Sorenson, Rev. Mod. Phys. **35**, 853 (1963).